In Situ ^{13}C Solid-State NMR and Ex Situ GC–MS Analysis of the Products of *tert*-Butyl Alcohol Dehydration on H-ZSM-5 Zeolite Catalyst

Alexander G. Stepanov,* Vladimir N. Sidelnikov, and Kirill I. Zamaraev*

Abstract: The hydrocarbon products that are formed upon dehydration at 296–673 K of *tert*-butyl alcohol (*t*BuOH), adsorbed on H-ZSM-5 zeolite in concentrations equal to that of active Al-OH-Si sites in the catalyst, have been analyzed by ^{13}C solid-state MAS NMR and GC–MS. To facilitate ^{13}C NMR analysis, the alcohol selectively labeled with ^{13}C isotope in the COH group was used. It was found that *t*BuOH transforms to the adsorbed C_8 butene dimers plus a trace amount of alkanes at 296 K. Butene dimers exist inside H-ZSM-5 pores in the form of interconverting adsorbed octene, octyl silyl ether, and octyl carbenium ion; octyl silyl ether is the main adsorption state. Fluxionality of the carbenium ion form provides a pathway for isomerization of the highly branched hydrocarbon skeleton of the initial alcohol to the predominantly linear one in the adsorbed butene dimer. The driving force for the isomerization into the linear structure is the shape selectivity induced by the small size of the zeolite channels. At 373 K the adsorbed butene dimers further crack into species that contain an average of about 6.5 carbon atoms, in addition to further alkanes. At 448 K the adsorbed C_3–C_{7+} paraffins become the predominant hydrocarbon products observed with both in situ ^{13}C NMR and ex situ GC–MS. Simultaneously, a mixture of adsorbed polyenes is formed. According to ^{13}C CP/MAS NMR, polyenes exist in the zeolite pores in the form of rather stable cyclopentenyl cations. At 573–673 K adsorbed cyclopentenyl cations further transform into a mixture of condensed and simple aromatics and then into xylenes and toluene. Simultaneously, paraffins crack further to give mainly C_3–C_4 paraffinic species at 573 K and propane at 673 K.

Keywords
alcohols · cracking · dehydrations · isomerizations · NMR spectroscopy

1. Introduction

Dehydration of *tert*-butyl alcohol (*t*BuOH) on acidic-form zeolites has been extensively studied by in situ IR,[1–3] solid-state NMR (^{13}C, ^{2}H),[4–6] and GC kinetic methods.[3] Diffusion and molecular dynamics of both *t*BuOH and the reaction products in zeolite pores have also been studied.[3, 6] From all these and similar studies with other isomeric butyl alcohols[7, 8] the key features of reaction mechanism were elucidated, and, in particular, reaction intermediates as well as oligomeric products trapped in zeolite pores were partly though not completely characterized.

In this work we further clarify the dehydration pathways (including subsequent isomerization and cracking of hydrocarbon products) at 296–673 K for *t*BuOH adsorbed on zeolite H-ZSM-5 in concentrations equal to that of the active catalytic Al-OH-Si sites. Both the species initially formed in the catalyst pores *and* the products escaping into the gas phase are characterized simultaneously with in situ ^{13}C solid-state NMR and ex situ GC–MS. In particular, we observe paraffins that are known to be formed on zeolites from hydrocarbons and alcohols at 400–700 K (see, e.g., refs. [9–18]), and show that they start forming from *t*BuOH at significantly lower temperature.

[*] Dr. A. G. Stepanov, Prof. K. I. Zamaraev
Laboratory for the Studies of the Mechanisms of Catalytic Reactions
Boreskov Institute of Catalysis
Siberian Branch of the Russian Academy of Sciences
Prospekt Akademika Lavrentieva 5, Novosibirsk 630090 (Russia)
Telefax: Int. code +(3832)35-57-56
e-mail: kiz@catalysis.nsk.su
Dr. V. N. Sidelnikov
Analytical Laboratory, Boreskov Institute of Catalysis

2. Results

2.1. Thermodesorption and GC–MS Analysis: To analyze the products that can *desorb* from the zeolite intracrystalline void, thermodesorption experiments were carried out at three different temperatures. The products were desorbed from the zeolite at 373 K, accumulated in a condenser, separated by gas chromatography (GC), and then analyzed by mass spectrometry (MS) (see Fig. 1 and description of the thermodesorption experiments in Experimental Section). The only detected product was isobutane (Fig. 2A). A similar experiment at 296 K showed no organic compound desorbing from the zeolite. At 448 K (Fig. 2B), C_4–C_7 paraffins were the main products. Note that our GC–MS analysis does not allow us to quantitatively assess the distribution of paraffins desorbing from the zeolite, nor does it give us any information about their structure (linear or branched). Moreover, it should be stressed here that the distribution and the structure of the volatile products *escaping* into a gas phase and identified by ex situ GC–MS analysis can be different to that of the organics remaining inside the zeolite pores.[14] The organic products that are *trapped* inside zeolite intracrystalline void can, however, be monitored in situ by means of ^{13}C MAS NMR spectroscopy.[14]

  0947-6539/96/0202-0157 $ 10.00+.25/0

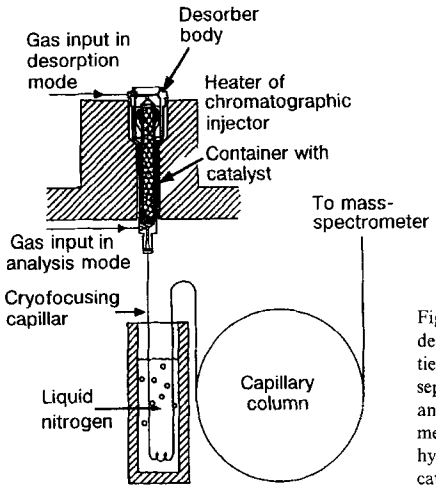

Fig. 1. Sketch of the thermodesorption apparatus with facilities for gas chromatographic separation on a capillar column and subsequent mass spectrometric analysis (GC–MS) of the hydrocarbons desorbed from the catalyst.

2.2. ^{13}C NMR Analysis: In principle, the known ^{13}C chemical shifts for the CH_n groups with various n ($n = 0-3$) in the liquid state can be used to identify hydrocarbons inside the zeolite channels,[19] since such shifts change only slightly (by 1–2 ppm[20]) upon adsorption into a zeolite. Unfortunately, for aliphatic hydrocarbon fragments, the positions of the ^{13}C signals from the CH_n groups with various n often overlap.[19] Therefore, to facilitate the assignment of the observed ^{13}C CP/MAS (cross-polarization magic-angle spinning) NMR signals, we used the two-dimensional (2D) J-resolved ^{13}C solid-state NMR spectroscopy. The advantage of this method[21] is that it yields information on both the ^{13}C chemical shifts ($F2$ dimension) and multiplicities, arising from scalar couplings of ^{13}C nuclei with the attached protons [$J(^{13}C-^{1}H)$ couplings] ($F1$ dimension). One can reliably attribute carbon signals to CH_n groups with a particular value of n by simply counting the number of lines in the corresponding multiplet signal.

Abstract in Russian:

Аннотация: Методами ЯМР высокого разрешения в твердом теле на ядрах углерода ^{13}C и газовой хромато-масс-спектрометрии (ГХМС) проанализированы углеводородные продукты, образующиеся в интервале температур 296-673 К при дегидратации *трет*-бутилового спирта (*t*-BuOH), адсорбированного на цеолит H-ZSM-5 в концентрации, равной концентрации активных в катализе Al-OH-Si центров. Для облегчения ^{13}C ЯМР анализа был использован спирт, селективно меченный изотопом ^{13}C в СОН группе. Найдено, что при 296 К *t*-BuOH превращается в адсорбированные на цеолите димеры бутена C_8 плюс следовые количества алканов. Димеры бутена существуют внутри пор цеолита H-ZSM-5 в виде трех взаимопревращающихся форм: октена, октил-силильного эфира и октильного карбениевого иона, причем октил-силильный эфир является доминирующим адсорбционным состоянием. Динамичность карбений-ионной формы обеспечивает изомеризацию сильно разветвленного углеводородного скелета исходного спирта в сторону образования димера бутена линейного строения. Движущей силой избирательной изомеризации в сторону образования линейного димера является малый размер каналов цеолита. При 373 К адсорбированные димеры бутена подвергаются дальнейшему крекингу в углеводородные фрагменты, содержащие в среднем 6,5 атомов углерода плюс дополнительное количество алканов. При 448 К адсорбированные парафины C_3-C_{7+} становятся преобладающими углеводородными продуктами, которые легко идентифицируются, как при помощи *in situ* ^{13}C ЯМР, так и при помощи *ex situ* ГХМС. Одновременно образуется смесь полиенов, остающихся адсорбированными на цеолите. Согласно ^{13}C ЯМР, полиены существуют в порах цеолита в виде стабильных циклопентадиенильных катионов. При 573-673 К адсорбированные циклопентадиенильные катионы подвергаются дальнейшим превращениям в смесь конденсированной и простой ароматики и затем в смесь ксилолов и толуола. Одновременно, парафины подвергаются дальнейшему крекингу с образованием преимущественно парафинов состава C_3-C_4 при 573 К и пропана при 673 К.

Editorial Board Member:[*] *Kirill I. Zamaraev was born in Moscow, Russia, in 1939. He received a BSc from the Moscow Institute of Physics and Technology (MIPT) in 1963 and was awarded a PhD in chemical physics in 1966 and a DSc in physical chemistry in 1972 by the Institute of Chemical Physics (ICP) in Moscow, which he left in 1976. From 1974 to 1975 he was a visiting researcher at Cornel and Stanford Universities and the University of Chicago. In 1977 he joined the Institute of Catalysis (now the Boreskov Institute of Catalysis) in Novosibirsk as Deputy Director. From 1984 until April 1995 he was Director of this Institute, when he became the Director of Research and Development of the Boreskov Institute of Catalysis. He has also been Professor of Chemistry and the Chairman of the Department of Physical Chemistry at the Novosibirsk State University since 1977. He was elected a Full Member of the Academy of Sciences of the USSR (now of Russia) in 1987 and to the President of IUPAC in 1993.*

Prof. K. I. Zamaraev's research interests include mechanistic studies of catalysis and, in particular, the characterization in situ with NMR and EPR of catalyst active sites and intermediates of catalytic reactions in solutions and on solid surfaces; the study of chemistry in the second coordination sphere of metal complexes; studies into the photochemistry and design of catalytic convertors for solar energy utilization; the kinetic characterization of numerous novel electron tunneling reactions; the study of the fundamentals of spin exchange in solution and its applications in chemistry.

[*] Members of the Editorial Board will be introduced to the readers with their first manuscript.

0947-6539/96/0202-0158 $ 10.00+.25/0 Chem. Eur. J. 1996, 2, No. 2

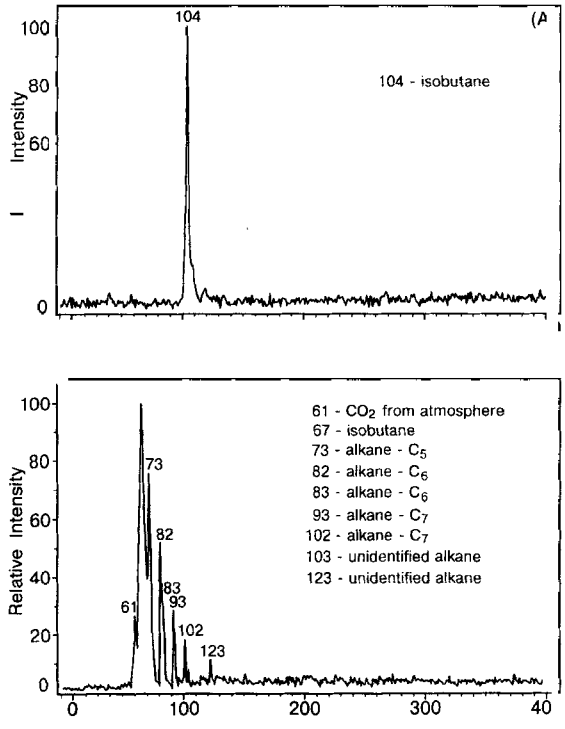

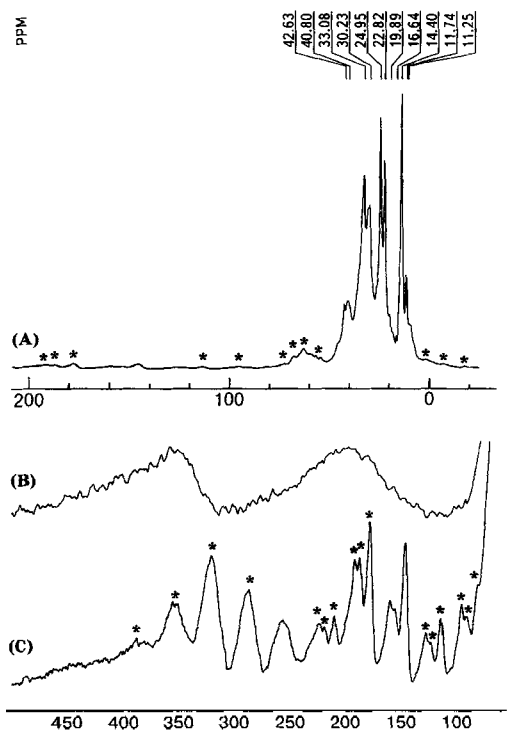

Fig. 3. ^{13}C CP NMR spectra of the products of [2-^{13}C]*t*BuOH dehydration on H-ZSM-5 zeolite at 448 K. (A) $\delta = 0-200$ region; the spectrum was recorded with MAS of the zeolite sample with adsorbed alcohol, 16500 scans. (B) and (C) 16-fold magnification of signal intensities relative to (A) for $\delta = 100-500$; (B) static spectrum, 14900 scans; (C) spectrum recorded with magic-angle spinning at a rate of 3.2 kHz. Asterisks denote spinning sidebands.

2.2.1. Analysis of hydrocarbons formed at high temperatures (448–673 K): First, we analyzed products that are formed at elevated temperatures (448, 573 and 673 K), since their ^{13}C NMR spectra contain less signals and are simpler to interpret. Moreover, some signals observed at elevated temperatures are also observed at lower temperatures (296 and 373 K). Their preliminary assignment to certain products helps in the analysis of the more complicated spectra at lower temperatures.

Assignment of ^{13}C NMR signals to hydrocarbons formed at 448 K: We already know from the thermodesorption experiment (vide supra) that a mixture of C_4-C_7 paraffins is formed on H-ZSM-5 zeolite at 448 K. Therefore, at least some of the ^{13}C NMR signals that were observed earlier for the products of *t*BuOH dehydration at 448 K[4, 5] may be ascribed to paraffins, rather than aliphatic fragments of butene oligomers as we assumed earlier.[5]

^{13}C CP/MAS NMR spectrum of the products of [2-^{13}C]*t*BuOH[22] dehydration on H-ZSM-5 zeolite at 448 K is shown in Figure 3A. Note, however, that the relative intensities of the signal integrals in this spectrum do not correspond to the contents of the various CH_n groups, because of the peculiarities of recording of ^{13}C NMR spectra with cross-polarization techniques.[23]

To resolve the multiplicities of carbon signals in the spectrum of Figure 3A, the 2D *J*-resolved ^{13}C NMR spectrum was recorded for the same sample. Figure 4A represents a contour plot of the 2D *J*-resolved spectrum. The one-dimensional spin-echo spectrum is given above the contour plot (Fig. 4B). From Figure 4A it can be seen that all the signals at $\delta = 8.1-25.5$

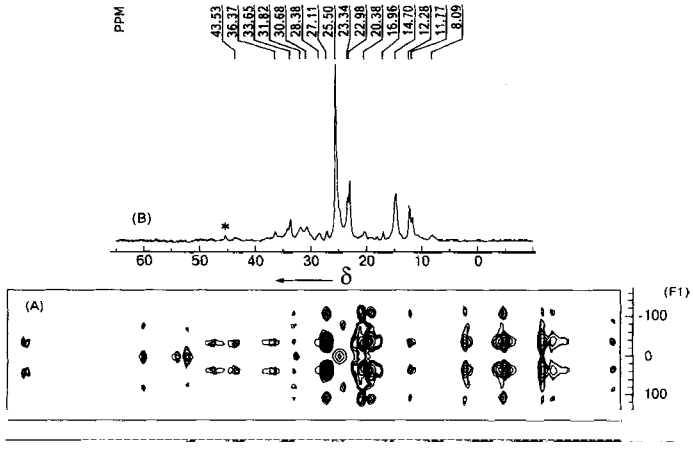

Fig. 4. (A) Contour plot of 2D *J*-resolved ^{13}C solid-state MAS NMR spectrum for the products of [2-^{13}C]*t*BuOH dehydration on H-ZSM-5 zeolite at 448 K. The observed value of scalar $J(^{13}C^{-1}H)$ coupling is equal to a half the real $J(^{13}C^{-1}H)$, because of proton high-power decoupling during the second half of the evolution time t_1 [21]. (B) One-dimensional ^{13}C MAS spin-echo NMR spectrum. Asterisk denotes a spinning sideband.

represent quartets (with the exception of the signal at $\delta = 24.5$) with $J(^{13}C^{-1}H) = 140 \pm 16$ Hz, and they can therefore be assigned to CH_3 groups.[24] The signals at $\delta = 28.4$, 30.7, 31.8, and 43.5 are doublets and should therefore be attributed to CH groups. The triplet structure of the signals at $\delta = 24.5$, 33.7, and 36.4 points to the presence of CH_2 resonances at these positions. The signal at $\delta = 34.2$ is a singlet or, possibly, triplet that is unresolved because of its low intensity. This signal should be

attributed to either a quaternary carbon atom or CH_2 group. The signal at $\delta = 27.1$ represents a superposition of a triplet and quartet and should therefore be ascribed to a sum of CH_3 and CH_2 groups.

To assess quantitatively the relative peak areas for various CH_n signals, one-dimensional one pulse excitation ^{13}C MAS NMR spectrum was recorded (Fig. 5A). Further, we have simulated the experimental spectrum of Figure 5A to derive peak areas. The experimental spectrum, which is given in Figure 5A, can be approximated by a superposition of 25 signals (Figs. 5B, C). Note that some of the signals in Figure 5A were not detected in the 2D *J*-resolved ^{13}C NMR spectrum (Fig. 4). This can be explained in terms of the peculiarities of recording 2D spectra, where spin-echo pulse sequence is used.[21] In spin-echo experiments the signals with short T_2 (slow molecular motion), that is, large line widths, may be undetectable. We therefore did not resolve the multiplicities of the signals with short T_2, which may belong to hydrocarbons of high molecular weight.

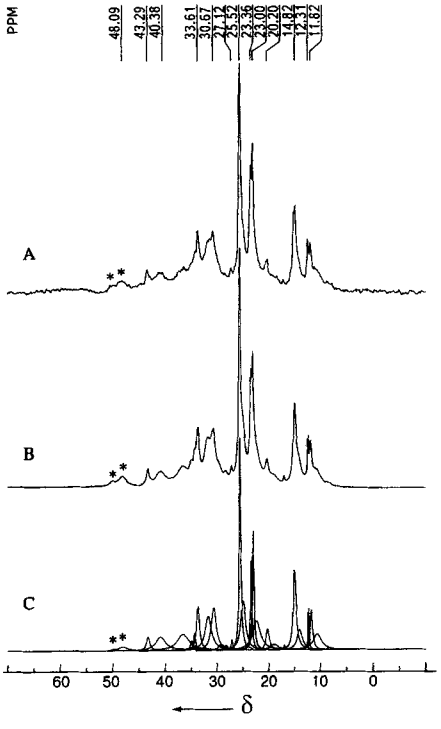

Fig. 5. (A) Experimental one pulse excitation ^{13}C MAS NMR spectrum with high-power proton decoupling for the products of [2-^{13}C]*t*BuOH dehydration on H-ZSM-5 zeolite at 448 K, 2100 scans. (B) Simulation of the experimental spectrum, with the superposition (C) of 25 signals from 11 paraffinic hydrocarbons (see Table 1). Asterisks denote spinning sidebands.

It should be remembered that in all our ^{13}C NMR studies *t*BuOH selectively labeled with the ^{13}C atom in the COH group, [2-^{13}C]*t*BuOH, was used. However, even at room temperature and all the more at elevated temperatures, this selectively introduced ^{13}C atom becomes scrambled randomly between various groups of both the initial alcohol and reaction intermediates and products.[5] (See, for example, the assignments of the ^{13}C CP/MAS spectra at $\delta = 10-40$ in Figs. 1 and 3 of ref. [5] for the dehydration products formed at 296 K from *t*BuOH, selectively labeled with ^{13}C in ^{13}COH or $^{13}CH_3$ groups). Therefore, our one-dimensional one pulse excitation ^{13}C MAS NMR spectra can indeed be used for the quantitative assessment of the relative amount of various hydrocarbon fragments and molecules inside the zeolite pores.

By comparing the chemical shifts and multiplicities of the signals observed for the reaction products at 448 K with those for liquid alkanes,[19] and by taking into account the relative peak areas, we assign the spectra in Figure 5 to a mixture of 11 saturated hydrocarbons, containing isobutane, isopentane, pentane, and C_{7+} paraffins as well as butene oligomers as the major fractions (see the assignment of the ^{13}C NMR signals and relative concentrations of the hydrocarbons in Table 1). Note that, according to ref. [25], for one of the expected products of *t*BuOH dehydration, namely, oct-1-ene adsorbed in H-ZSM-5, the signals from the >C=C< moiety are not detected in the ^{13}C NMR spectra (presumably, because of broadening due to the exchange phenomena), while those from all other CH_n groups are clearly observed.[25] We therefore only observe the signals from the aliphatic fragments of the adsorbed octenes and higher butene oligomers (remember that isobutene is one of the primary products of *t*BuOH dehydration on H-ZSM-5), together with the signals from a mixture of paraffins.

We next turned to the identification of the ^{13}C NMR signals at $\delta = 100-400$. ^{13}C CP NMR spectrum of hydrocarbons formed from *t*BuOH at 448 K also exhibits two broad lines around $\delta = 200$ and 350 (nonspinning sample, Fig. 3B). Magic-angle spinning of this sample revealed that these broad lines are

Table 1. Assignment of ^{13}C NMR signals and concentrations (mol%) [a] for paraffins, butene oligomers, and aromatics formed from *t*BuOH on H-ZSM-5 at 373–673 K.

	Chemical shifts [b]					Concentration			
	*CH_3-	-*CH_2-	*CH_3-CH-CH_3	-*CH<	-*C-	373 K	448 K	573 K	673 K
ethane	7.5 (5.7) [b]								8.7
propane	17.0 (15.4)	18.0 (15.9)				<1	1.0	29.8	59.2
n-butane	14.7 (13.1)	27.1 (24.9)					<1.7	18.5	5.3
isobutane			25.5 (24.3)	25.5 (25.0)		6	17.2	19.6	5.3
n-pentane	14.7 (13.7)	24.5, 36.6 (22.6, 34.6)					17.2	3.7	
isopentane	11.8 (11.4)	33.6 (31.7)	23.0 (21.9)	30.7 (29.7)		5	17.9	11.7	
neopentane				27.1 (27.4)	31.8 (31.4)		0.7		
n-hexane	14.7 (13.7)	24.5, 33.7 (22.8, 31.9)					6.9		
2-methylpentane	14.7 (14.0)	20.2, 40.9 (20.5, 41.6)	23.5 (22.4)	28.4 (27.6)		7	4.1		
2,3-dimethylbutane			20.2 (19.1)	34.9 (33.9)			3.4		
2,2-dimethylbutane	8.5 (8.5)	36.6 (36.5)	29.6 (28.7)		30.7 (30.2)		2.1		
C_{7+} paraffins + butene oligomers	10.6, 11.8 13.9	22.3, 23.4, 30.7, 34.2, 36.6, 40.9		43.4, 30.7		82	27.8		
o- and *p*-xylenes	20.7 (19.6, 20.9)							16.7 [c]	13.4 [c]
toluene + *m*-xylene	22.5 (21.3)								8.1 [c]

[a] With respect to the total amount of CH_n groups with signals between $\delta = 10$ and 40. [b] The chemical shifts of CH_n groups of adsorbed hydrocarbons presented here are taken from Figures 3–11; accuracy of the δ measurement is ± 0.5 ppm; the chemical shifts of hydrocarbons in solution (from ref. [19]) are given in parentheses. [c] These values only take into account the amount of CH_3 carbon and not the amount of carbon in the benzene ring.

0947-6539/96/0202-0160 $ 10.00+.25/0 Chem. Eur. J. 1996, 2, No. 2

superpositions of four anisotropic signals with the isotropic chemical shifts at $\delta = 145$, 155, 159, and 254[26] (Fig. 3C). The isotropic signal at $\delta = 254$ is indicative of a trivalent carbon atom in a carbenium ion center of allyl[27] or cycloalkenyl[28] cations. The isotropic signals at $\delta = 145-159$ can be attributed to carbon atoms adjacent to the carbenium ion center in these cations. The simultaneous disappearance at 573 K of both the signals at $\delta = 145-159$ and the signal at $\delta = 254$ (vide infra) supports our suggestion that the two groups of signals belong to the same species. The observed set of signals can not be attributed to simple allyl cations, since the latter are not persistent inside acidic zeolites.[29, 30] This set of signals best matches that for a mixture of the adsorbed alkyl-substituted cyclopentenyl cations with symmetrically disposed alkyl fragments around the carbenium ion center, such as 1,2,3-trimethylcyclopentenyl cation (the shifts in solution are $\delta = 247$ and 155[28]), 1,3-dimethylcyclopentenyl cation (the shifts in solution are $\delta = 249$ and 148[31]), and similar cations with alkyl substituents other than methyl groups ($\delta = 254$ and 150 in Fig. 3C). Note that similar ^{13}C NMR signals from cyclopentenyl cations inside zeolites have already been observed earlier by Haw et al.[16, 32] According to the same authors, cations of this type can also be generated in high yield on acidic zeolites from cyclic[33] or aromatic[34] precursors.

Assignment of ^{13}C NMR signals to hydrocarbons formed at 573 K: Heating of the zeolite sample with adsorbed *t*BuOH at 573 K results in a redistribution of the signal intensities in the region of $\delta = 10-40$ (compare Figs. 3A and 6). Now the signals from C_3-C_5 paraffins are mainly observed, with propane and butanes as the predominant products (see Table 1).

In the region of $\delta = 100-300$ the signals from cyclopentenyl cations have now practically disappeared (compare spectra in Fig. 3C and Fig. 6B). A weak signal at $\delta = 145$ may correspond to trace quantities of this cation. The main signals observed above $\delta = 100$ (Fig. 6B) are now those with the isotropic chemical shifts $\delta = 129$ (the most intense signal), $\delta = 127$ (seen as a shoulder of the signal at $\delta = 129$), and the signals of essentially lesser intensity with isotropic shifts $\delta = 137$, 139, and 147. Such isotropic chemical shifts are typical for simple and condensed aromatics.[19] The range of shifts is known to be narrower for condensed aromatics (e.g., $\delta = 125-131$ for pyrene in solution[19]) than for simple ones (e.g., $\delta = 126-138$ for liquid xylenes[19]).

Though one cannot conclude unambiguously whether the signals at $\delta = 127-139$ belong to simple or condensed aromatics, or to a mixture of both, it is tentatively possible to assign the most intense signal at $\delta = 129$ to a superposition of lines from adsorbed condensed aromatics and the weak but clearly detectable signals at $\delta = 127$, 137, and 139 to adsorbed simple aromatics, such as xylenes. The formation of xylenes is also supported by the presence in the spectrum of Figure 6A of the signal at $\delta = 20$, which certainly does not belong to paraffins and is indicative of methyl groups attached to a benzene ring. Numerous spinning sidebands observed for the signals of aromatics and cyclopentenyl cations (vide supra) show that these species are rather immobile inside the zeolite channels. Relative amounts of various hydrocarbons formed at 573 K are given in Table 1.

Assignment of ^{13}C NMR signals to hydrocarbons formed at 673 K: Heating of the zeolite with adsorbed alcohol at 673 K results in a further increase in the amount of lighter paraffins inside the zeolite. A new signal at $\delta = 7.5$ from ethane appears, and the main signal observed at $\delta = 10-40$ arises from propane (see Fig. 7 and Table 1). Rather narrow and compactly disposed signals at $\delta = 127-139$ indicate the formation of a mixture of simple aromatic compounds. According to their chemical shifts, the signals at $\delta = 20.7$, 22.4, and 127–139 can be assigned to a mixture of *o*-, *p*-, *m*-xylenes and toluene.[19] Relative amounts of hydrocarbons formed at 673 K are given in Table 1.

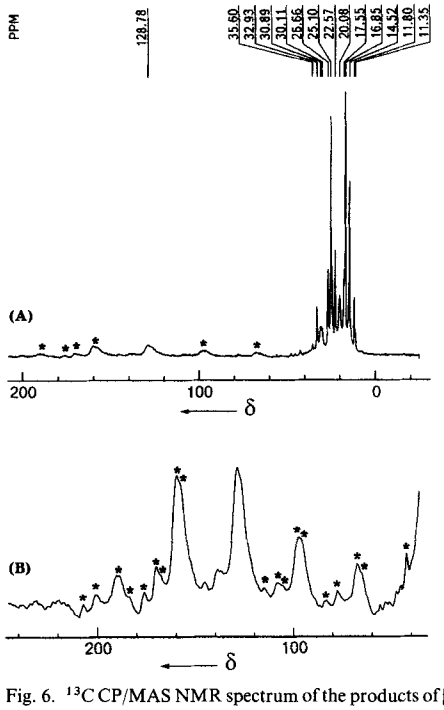

Fig. 6. ^{13}C CP/MAS NMR spectrum of the products of [2-^{13}C]*t*BuOH dehydration on H-ZSM-5 zeolite at 573 K, 3000 scans. (A) Region of $\delta = 10-200$; (B) 8-fold magnification of signal intensities in the region of $\delta = 40-240$. Asterisks denote spinning sidebands.

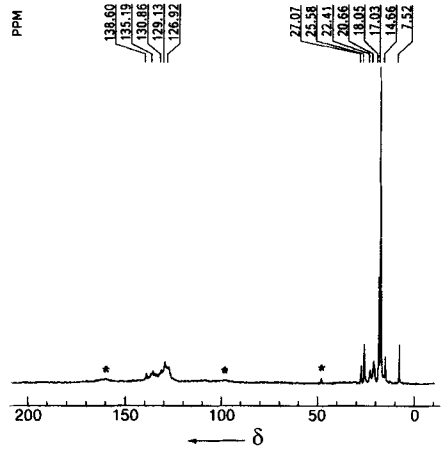

Fig. 7. ^{13}C MAS NMR spectrum of the products of [2-^{13}C]*t*BuOH dehydration on H-ZSM-5 zeolite at 673 K, 700 scans. Asterisks denote spinning sidebands

Note, that the total amount of aromatics increases with increasing reaction temperature. At 573 K the overall intensity of the signals from aromatics in the regions of $\delta = 10-40$ and 120–140 are about 40% of that from paraffins, while at 673 K the overall intensities are approximately equal. Thus, the increase of the reaction temperature favors cracking of paraffins to a lighter species, on the one hand, and formation of aromatics, on the other. A similar trend has been observed many times by ex situ methods for conversion of various hydrocarbon feedstocks on zeolites (see, e.g., refs. [9–18]).

2.2.2. Analysis of hydrocarbons formed at low temperatures (296–373 K):

Assignment of ^{13}C NMR signals to hydrocarbons formed at 373 K: Figure 8A shows ^{13}C CP/MAS NMR spectrum of the products of [2-^{13}C]*t*BuOH dehydration at 373 K. At first glance, the spectra for the products formed at 373 K and 448 K are similar (compare Figs. 3A and 8A), except that the spectrum for 373 K contains an additional small signal at $\delta = 86$ for the previously identified *tert*-butyl silyl ether.[5] However, our attempts to record 2D *J*-resolved ^{13}C NMR spectra for the dehydration products formed at 373 K were not successful. In the spin-echo spectrum (used in 2D NMR experiment[21]) recorded for these products with $t_1 = 0.5$ ms, some signals observed for the hydrocarbons formed at 448 K are absent, and the common signals exhibit a different distribution of intensities (compare Fig. 9A and B). We attribute these experimental facts to a rather short relaxation time T_2 (0.3–0.6 ms) for CH_2 groups of the reaction products. Short values of T_2 for CH_2 fragments indicate that hydrocarbon species formed at 373 K exhibit low molecular mobility inside the zeolite and may therefore represent adsorbed long-chain oligomers or paraffins, rather then the short-chain paraffins that have been observed by ^{13}C NMR at more elevated temperatures (vide supra). Indeed, according to ^{2}H NMR, for butene oligomers formed from deuterated *t*BuOH at 373 K, the correlation time for the isotropic reorientation at 296 K is $\tau_c > 10^{-6}$ s.[6] If one assumes that carbon ^{13}C relaxation times (T_1, T_2) of the adsorbed oligomers are governed mainly by the dipolar mechanism,[35] then one can estimate that at the magnetic field of 9 Tesla, T_1 should be of the order of few seconds and $T_2 \approx 0.1$ ms. This means that for the spin-echo spectrum, recorded with $t_1 = 0.5$ ms, the intensity of the signals from CH_2 groups should be of the order of several percent, compared to the same signal expected for the usual one pulse excitation sequence. Therefore, the signals from fast rotating methyl groups with $\tau_c \approx 10^{-10}$ s[36] and $T_2 \approx 1-4$ ms dominate at $\delta = 14-25$ in the spin-echo spectrum for the sample heated at 373 K (Fig. 9B). However, signals from the groups other than CH_3 are clearly visible and even dominate in the one pulse excitation ^{13}C MAS NMR spectrum for the same sample (Fig. 8B).

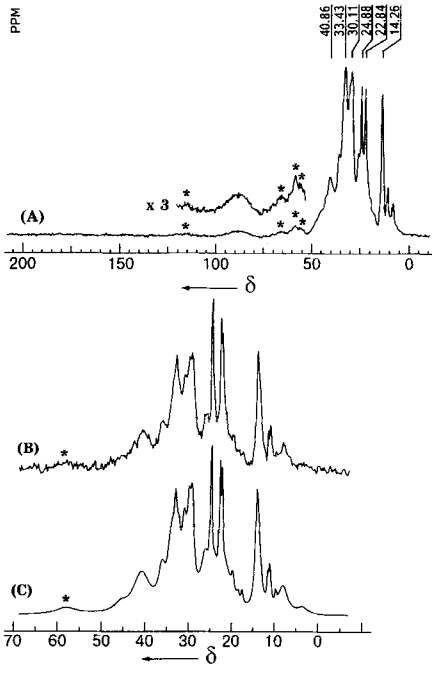

Fig. 8. (A) ^{13}C CP/MAS NMR spectrum of the products of [2-^{13}C]*t*BuOH dehydration on H-ZSM-5 zeolite at 373 K, 9300 scans, $\delta = 10-200$. (B) Experimental one pulse excitation ^{13}C MAS NMR spectrum with high-power proton decoupling of the hydrocarbon products for the same zeolite sample. (C) Simulation of the experimental spectrum with the superposition of the signals from the adsorbed butene dimers and paraffins. Asterisks denote spinning sidebands.

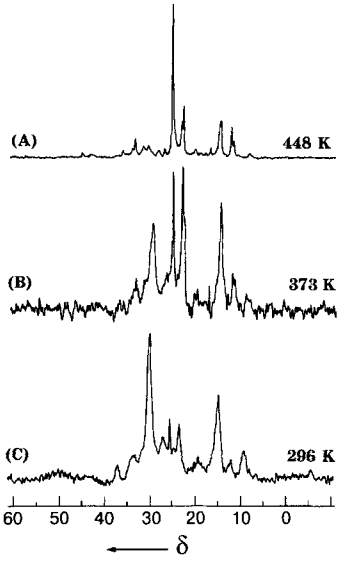

Fig. 9. ^{13}C MAS spin-echo NMR spectra of the products of [2-^{13}C]*t*BuOH dehydration on H-ZSM-5, formed at different temperatures. Spectra were recorded with the pulse sequence described in the Experimental Section) and $t_1 = 0.5$ ms. (A) 448 K, 1200 scans; (B) 373 K, 800 scans; (C) 296 K, 10000 scans.

The arguments mentioned above do indeed suggest that oligomeric species with longish hydrocarbon chains are the main products at 373 K. However, short-chain alkanes are also formed in small amount. Indeed, on the one hand thermodesorption experiment reliably shows the formation of isobutane at 373 K (Fig. 2A); on the other hand, the positions of sharp signals at $\delta = 10-25$ in Figure 9B from the methyl groups coincide with those for the CH_3 groups of alkanes identified at 448 K (vide supra). We therefore conclude that some of the paraffinic species are formed at 373 K.

To quantitatively estimate the amount of various species formed at 373 K, we have simulated the experimental one pulse excitation spectrum of Figure 8B in the same way as for the sample heated at 448 K (vide supra). Simulations (Fig. 8C) show that the experimental spectrum (Fig. 8B) can be satisfactorily approximated by a superposition of the signals from propane, isobutane, isopentane, 2-methylpentane, and two types of long-chain oligomers (linear oligomers and branched oligomers with the terminal $(CH_3)_2CH$ fragments). In simulations the chemical shifts indicated in Table 1 were used for the alkanes. The following values were taken as the shifts for long-chain oligomers:[19, 38] 1) linear species: $\delta = 10-14.7$ (CH_3 terminal), 22–26 (CH_2 next to CH_3), and 30–35 (inner CH_2); 2) branched species: $\delta = 22-26$ for CH_3 and 30–40 for CH groups of the $(CH_3)_2CH$ fragment. For oligomers the following ratios for the amounts of various groups were found: CH_3:CH_2 (adjacent):CH_2 (inner):$(CH_3)_2CH = 1:1:2.5:0.34$. Thus, our analysis shows that hydrocarbons with linear chains are preferentially formed from *t*BuOH at 373 K. The distribution of the various paraffins formed from *t*BuOH at 373 K are shown in Table 1. All together they make up about 18% of the total hydrocarbon fragments exhibiting NMR signals at $\delta = 10-40$. The remaining 82% of carbon atoms belong to oligomers.

Assignment of ^{13}C NMR signals to hydrocarbons formed at 296 K: *t*BuOH was reported to undergo a slow dehydration on H-ZSM-5 zeolite to form butene oligomers and water even at room temperature.[1–6] Figure 10A shows the ^{13}C CP/MAS NMR spectrum of [2-^{13}C]*t*BuOH that was recorded four hours after adsorption at 296 K. The less intense signal at $\delta = 81.6$ from the initial unchanged alcohol with the labeled ^{13}COH group and the more intense signals at $\delta = 10-40$ from butene oligomers dominate this spectrum. The signal from the *tert*-

0947-6539/96/0202-0162 $ 10.00+.25/0 Chem. Eur. J. 1996, 2, No. 2

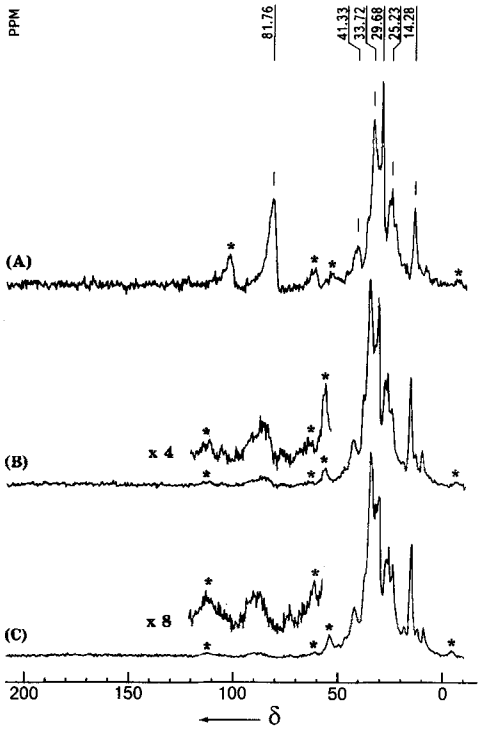

Fig. 10. ^{13}C CP/MAS NMR spectra of [2-^{13}C]*t*BuOH adsorbed on H-ZSM-5 zeolite at 296 K. (A) 4 h after adsorption, 2200 scans; (B) 24 h after adsorption, 5800 scans; (C) 48 h after adsorption, 15000 scans. Asterisks denote spinning sidebands.

butyl silyl ether, *t*BuSE,[5] is also visible in this spectrum as a shoulder at around $\delta = 86$. After this sample had been kept at 296 K for 24 hours, the signal at $\delta = 86$ from *t*BuSE was clearly visible, while the sharper signal at $\delta = 81.6$ from the initial alcohol could hardly be made out against the background of the broad signal at $\delta = 86$ (Fig. 10B).

Note the appearance of a sharp signal at $\delta = 29.7$ among the signals from butene oligomers. This signal corresponds to the CH_3 group of [2-^{13}C]*t*BuOH, which is formed from [2-^{13}C]*t*BuOH as a result of scrambling of the ^{13}C label between the COH and CH_3 groups by a reversible reaction inside the zeolite [Eq. (a)].[5] The signals at $\delta = 29.7$ from the unchanged

$$[2\text{-}^{13}C]t\text{BuOH} \rightleftharpoons t\text{Bu}^+ + \text{HO}^- \rightleftharpoons [1\text{-}^{13}C]t\text{BuOH} \quad \text{(a)}$$

alcohol are also observed 24 hours after adsorption (Fig. 10B). This is an additional piece of evidence for the slowness of *t*BuOH dehydration on H-ZSM-5 at 296 K. Note that the rate of dehydration increases with increasing Si/Al ratio in the zeolite. For example, in the sample with Si/Al = 29 the dehydration was reported to be complete within 15 hours,[5] notably faster than for the sample with Si/Al = 44 used in this work.

To estimate the relative amounts of the various fragments in the butene oligomers formed at 296 K, we have simulated (Fig. 11B) the experimental one pulse excitation spectrum of Figure 11A, recorded 48 hours after *t*BuOH adsorption. The following ratios were obtained: CH_3 (terminal linear):CH_2 (adjacent):CH_2 (inner):$(CH_3)_2CH = 1:1:3.9:0.31$. This ratio pattern is very close to the ratio of 1:1:4:0.27 previously reported for oct-1-ene (with the natural ^{13}C abundance) adsorbed on H-ZSM-5 zeolite at 290 K[25] (see also Section 3.1. for additional clarification of this ratios pattern). Thus, the decrease of temperature from 373 K to 296 K leads to a slight decrease in the amount of branched $(CH_3)_2CH$ fragments and to an increase in the average length of the hydrocarbon chain in oligomers up to about eight carbon atoms. It is interesting that linear chains dominate over branched ones in oligomers, despite the fact that the initial alcohol contains a highly branched hydrocarbon fragment.

We failed to record 2D *J*-resolved ^{13}C NMR spectra for the CH_2 groups of the hydrocarbon products formed at 296 K, for the same reason as for $T = 373$ K (vide supra), namely, low molecular mobility and too short values of $T_2 \approx 0.1$ ms. Indeed, the spin-echo spectrum (recorded with $t_1 = 0.5$ ms, Fig. 9C) exhibits a notably lower signal-to-noise ratio than that at 448 K (Fig. 9A), in spite of the tenfold increase in the number of free induction decays (FIDs) accumulated before Fourier transformation. The signals from fast rotating methyl groups with relatively long $T_2 \approx 1$ ms are mainly observed. Analysis of ^{13}C NMR signals in the spin-echo spectrum of Figure 9C and one pulse excitation spectrum of Figure 11 suggests that the same paraffinic products are formed at 296 K as at 373 K, namely, isobutane (signal from methyl groups at $\delta = 25.5$) and also perhaps isopentane (the signals from methyl groups $\delta = 11.8$ and 23.4) as well as 2-methylpentane (the signals from methyl groups at $\delta = 14.7$ and 23.4), though in quite small amount.

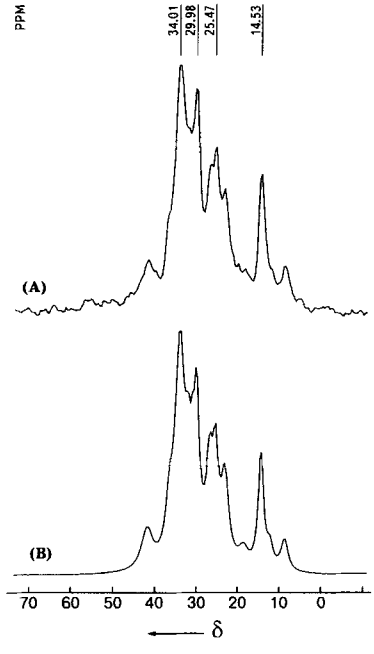

Fig. 11. Quantitative estimation of relative peak areas in the ^{13}C MAS NMR spectrum for the hydrocarbon products formed from [2-^{13}C]*t*BuOH at 296 K. (A) Experimental one pulse excitation spectrum, 3300 scans. (B) Simulation of the experimental spectrum.

3. Discussion

On the basis of previous GC and IR kinetics as well as NMR studies, the pathways shown in Scheme 1 for dehydration of

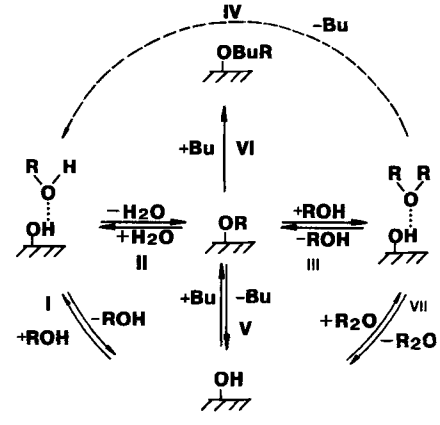

Scheme 1. The pathways for the conversion of butyl alcohols on zeolite H-ZSM-5 according to refs. [3,5,7,8].

*t*BuOH and other isomeric butyl alcohols inside the pores of H-ZSM zeolite were proposed.[3, 5, 7, 8] Note that stages III and VII were not elucidated for *t*BuOH, but for other less bulky butyl alcohols. According to Scheme 1, butene oligomers bound to the zeolite lattice (-OBuR) are among the reaction products. NMR data obtained in ref. [25] and this paper shed further light on the nature, composition, structure, and further transformations of the adsorbed oligomers within the zeolite pores.

3.1. The Nature of Adsorbed Butene Oligomers: The characteristic signals from the olefinic >C=C< moiety are absent[3, 5] at $\tilde{\nu} = 1660-1670$ (C=C) and 3020–3090 cm^{-1} (=C–H) in the IR spectra[38] and at $\delta = 110-140$ in the ^{13}C NMR spectra.[19] At first glance, these results provide evidence that the oligomeric species exist as alkyl silyl ethers **2** or carbenium ions **3** rather than adsorbed olefins **1** (Scheme 2). However, in support to the earlier finding by van den Berg et al.[39] we have recently found[25] that oct-1-ene, which can be considered as one of the expected products of butene oligomerization, when adsorbed on H-ZSM-5, exhibits neither the characteristic signals of stable **3** at $\delta = 300-330$[40] (C^+ center) nor those at $\delta = 70-90$ from the C–O moiety of **2** in its ^{13}C NMR spectra.[5, 32, 41] At the same time the adsorbed oct-1-ene clearly exhibits[25] fluxionality that is typical for **3**.[42, 43] For example, a ^{13}C label initially located at the $=CH_2$ group of the olefinic moiety gradually scrambles over the entire hydrocarbon skeleton of oct-1-ene.[25]

The absence of the ^{13}C NMR signals from the characteristic moieties for **1**–**3** in adsorbed oct-1-ene over a wide temperature range (173–296 K) was rationalized[25] in terms of signal broadening as a result of slow or intermediate-rate (on the ^{13}C NMR timescale) interconversions shown in Scheme 2.

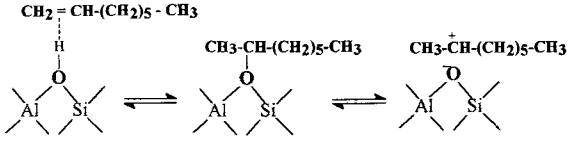

1 **2** **3**

Scheme 2. Interconversions of oct-1-ene adsorbed on zeolite H-ZSM-5.

Note, that hydrogen-bond complexes **1** between olefins and acidic OH groups of zeolites are indeed formed, as is known from IR data from 1966.[44] Alkyl silyl ethers **2** have been observed by NMR spectroscopy.[5, 32, 41] Evidence for the formation of carbenium ions **3** comes from the scrambling of the ^2H and/or ^{13}C label, initially introduced selectively into the active catalytic site or into the reactants (alcohols or hydrocarbons), over the entire hydrocarbon skeleton of the reacting molecules adsorbed on acidic zeolites.[2, 4–6, 25, 41, 45–48] This scrambling was observed by kinetic studies[49] and chemical trapping of adsorbed carbenium ions with carbon monoxide.[50]

The fact that **1**, **2**, and **3** cannot be observed by ^{13}C NMR spectroscopy, because of the slow or intermediate rate of the exchange process in Scheme 2 (vide supra), implies that the these adsorbed butene dimers should be observable by IR spectroscopy. Indeed, the characteristic timescale (ca. 10^{-13} s) of IR is many orders of magnitude shorter than that of ^{13}C NMR spectroscopy (ca. 10^{-4}–10^{-5} s). Therefore, the IR spectra would be expected to show separate nonaveraged signals for each of the species **1**–**3**. However, as mentioned above, the bands characteristic of the olefinic moieties in **1** are not observed in IR spectra of oligomeric products formed by *t*BuOH dehydration.[2, 3] This fact clearly indicates that the adsorbed butene oligomer is not present in any substantial amount in the form **1**. The absence of the signal in the IR spectrum from carbenium ions at $\tilde{\nu}^{as} = 1290-1300$ cm^{-1} (^+C-C)[51] for the products of *t*BuOH dehydration[2, 3] suggests that species **3** is also not the predominant form of oligomer adsorption in the H-ZSM-5 zeolite. However, a small fraction of butene oligomers must exist in form **3**, otherwise carbon scrambling for oct-1-ene in H-ZSM-5[25] cannot be explained.

Unfortunately, the characteristic IR lines of **2** at $\tilde{\nu} = 1055-1175$ cm^{-1} (C–O)[52] cannot easily be observed against the background of the substantially more intense band at $\tilde{\nu} = 1100$ cm^{-1} corresponding to ν(Si–O) of the zeolite framework.[53] Our failure to observe the ν(C–O) band of **2** with IR does not therefore prove that these species are not present in the zeolite in substantial amounts. Moreover, quantum-chemical calculations by Kazansky and Senchenya[54] indicate that species **2** should be a considerably more stable form of olefin adsorption on acidic zeolites than species **1** and **3**.

Thus, we come to the conclusion that **2** is most probably the main adsorption state for butene oligomers inside H-ZSM-5, but that it is certainly in equilibrium with species **1** and **3** (Scheme 2) in significantly smaller concentrations.

As mentioned above, the absence in our ^{13}C NMR spectra of the signals near $\delta = 70-90$ characteristic of species **2** can be rationalized in terms of its dynamic behavior. A simple mechanism that would account for the absence of a ^{13}C signal from the C-O-Si moiety is presented in Scheme 3. With an intermediate rate of exchange (on the ^{13}C NMR timescale), the signal in the vicinity of $\delta = 70-90$ is expected to be too broad to be visible.[55]

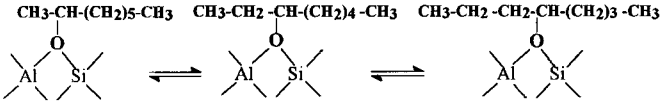

Scheme 3. A possible dynamic behavior of alkyl silyl ethers in acidic zeolite.

Thus, the whole set of available NMR, IR, and quantum-chemical data, when taken as a whole, suggest that olefin oligomers formed inside the channels of the H-ZSM-5 zeolite exist predominantly in the form of alkyl silyl ether **2**, which participates in the exchange processes shown in Schemes 2 and 3.

3.2. Composition and Structure of Adsorbed Butene Oligomers: Our data show that mainly linear rather than branched fluxional oligomers are formed both during *t*BuOH dehydration (vide supra) and oct-1-ene adsorption on H-ZSM-5. Indeed, the chemical shifts for the terminal CH_3, the adjacent CH_2, and further removed CH_2 groups, as well as the ratios of the intensities of their ^{13}C NMR signals for the adsorbed linear oligomers formed from *t*BuOH, practically coincide with the corresponding values for adsorbed oct-1-ene.[25] This means that linear butene oligomers formed from *t*BuOH are dimers, that is, C_8 species adsorbed inside H-ZSM-5 in the same way as oct-1-ene.

One can assume that the predominant formation of linear C_8 species from highly branched *t*BuOH is driven by the shape-selectivity effect induced by the narrow pore channels (ca. 5.5 Å[56]) in H-ZSM-5 and rapid isomerization (compared to the rate of dehydration) of the hydrocarbon skeleton in the carbenium ion form **3**. As the temperature increases from 296 K to 373 K, the average number of carbon atoms in the oligomer

0947-6539/96/0202-0164 $ 10.00+.25/0 Chem. Eur. J. 1996, 2, No. 2

decreases, from about 8 to about 6.5 (i.e., by ca. 18%), owing to cracking process. As expected, this value is the same as the percentage of carbon atoms that are transferred from oligomers to paraffins at 373 K (vide supra).

3.3. Transformations of Butene Dimers inside H-ZSM-5: The ^{13}C NMR data suggest that small amounts of light paraffins are formed as products at temperatures as low as 373 K and even 296 K under our reaction conditions, when concentrations of the reactants and products in the zeolite pores are close to that of the Al-OH-Si active site. Of course, one may argue that the quantitative analysis of our experimental NMR spectra in terms of a superposition of more than twenty lines from more than 10 different species is ambiguous. Indeed, although we found superpositions that fitted well with the experimental spectra, we cannot prove that they are the only ones that fit. Nevertheless, we feel that our conclusion about the formation of paraffins at low temperature is qualitatively correct. Indeed, the chemical shifts for some of the paraffins (such as propane and isobutane) are rather characteristic. Moreover, our thermodesorption GC–MS data clearly confirm the formation of isobutane at 373 K (Fig. 2A).

The suggested pathways for the transformation of butene dimers inside our H-ZSM-5 samples are shown in Scheme 4 (to simplify the scheme only linear species are shown). We think that paraffins are formed upon cracking (disproportionation) of

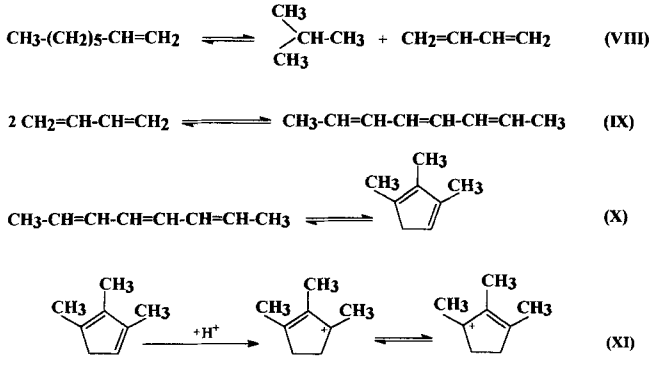

Scheme 4. The pathways of transformation of butene dimers on zeolite H-ZSM-5 at 296–448 K.

the adsorbed butene dimers through reaction (VIII). This conclusion is supported by the simultaneous increase in the amount of paraffins and decrease in the ratio of CH_2 (inner) to CH_3 (terminal linear) for the fluxional alkyl silyl ether from 3.9 at 296 K to 2.6 at 373 K. This corresponds to the decrease in the average number of carbon atoms in the hydrocarbon skeleton from about 8 to about 6.5.

According to the classic scheme for the cracking of high olefins on acidic solids,[57] diene hydrocarbons should be formed in reaction (VIII) together with paraffins. The signals from the dienes would be expected at around 1600 cm^{-1} in the IR[58] and at $\delta = 100-140$ (1,3-dienes) or $\delta = 70-90$ and 200–210 (allynes) in the ^{13}C NMR spectra,[19] at least at elevated temperature (448 K) where a significant proportion of the oligomers crack. However, numerous IR studies on the transformation as a function of temperature of oligomers formed from various olefins on H-ZSM-5 have shown that the band at $\tilde{\nu} \approx 1510$ rather than at 1600 cm^{-1} is usually observed,[1, 59–63] sometimes even at room temperature.[1] The intensity of the signal at 1510 cm^{-1} first increases with temperature, reaches its maximum at about 473 K, and then decreases.[63] This IR band was assigned either to ν(C=C) stretch in aromatic rings[59, 60, 62] or to $\tilde{\nu}^{as}$(CCC) in allylic carbenium ions.[61, 63] The ^{13}C NMR studies by Haw et al.[16, 32] and the data of this work suggest that the band at 1510 cm^{-1} should be attributed to cyclopentenyl cations. We assume that dienes formed in reaction (VIII) react rapidly, presumably via the triene species (reaction (IX)). Isomerization and cyclization (reaction (X)) and subsequent protonation (reaction (XI)) finally yield cyclopentenyl cations (see ^{13}C NMR spectra in Fig. 3). It should be mentioned that we have also observed (^{13}C NMR) the formation of the same cyclopentenyl cations on H-ZSM-5 at temperature above 373 K from *i*BuOH, *n*BuOH, oct-1-ene, and ethylene.

Thus literature data on the conversion of olefins and alcohols to paraffins and simple aromatics on acidic zeolites (IR: see, e.g., refs. [1, 59–63]; ^{13}C NMR: refs. [15, 16, 32, 64–66]) together with the data presented in this paper allow us to conclude that the formation of a stable cyclopentenyl cations is a common feature of such conversions. These cations are produced simultaneously with paraffins from oligomers. Their concentration increases with temperature and reaches its maximum at about 473 K.[63] At higher temperatures they gradually convert to aromatics, which have been identified on many occasions by ^{13}C NMR spectroscopy.[15, 16, 65, 66]

There is a remarkable similarity between the processes of olefin conversion (alcohol dehydration) on zeolites and in concentrated sulfuric acid. As far back as the 1870s Butlerov found the main products of butyl alcohol dehydration in sulfuric acid solutions to be butenes, butene oligomers (dimers), and dibutyl ethers.[67] As seen from Scheme 1 the same products are formed over a heterogeneous H-ZSM-5 catalyst.

In 1936 Ipatieff and Pines[68] revealed that in 96–98% sulfuric acid at 273 K olefins (other than ethylene and propylene) convert into a mixture of paraffins and cycloolefins. In the early sixties Deno et al.[69] showed, using NMR spectroscopy, that the latter exist in 96% H_2SO_4 in the form of stable cyclopentenyl cations.

3.4. Role of Fluxional Alkyl Silyl Ethers in Catalysis: In this paper we have intentionally studied *t*BuOH dehydration with very small concentrations of reagent (comparable to that of active Al-OH-Si sites in the zeolite). This helped us to minimize the background ^{13}C NMR signals from physisorbed reactants and products and thus to increase the visibility of the signals from the chemisorbed reaction intermediates.

tBuOH dehydration: Let us now discuss the expected behavior of the chemisorbed states characterized here, in reactions that proceed under more practical conditions, when the total concentration of reactant in the feedstock stream considerably exceeds that of active catalytic sites.

Under steady-state conditions in a flow system, dehydration of *t*BuOH on H-ZSM-5 zeolite at 296–333 K resulted in butenes and H_2O as the only compounds detected by GC in the product stream.[3] No paraffins were observed under these conditions. Fluxional octyl silyl ether remains trapped (chemisorbed) in the zeolite pores under these conditions. With its formation the catalytically active Al-OH-Si groups gradually disappear through the sequence of reaction steps I, II, VI and/or V, VI (see Scheme 1) and are converted to the octyl silyl ether. Thus, the active Al-OH-Si sites located in the pores become poisoned. This cannot be prevented by reaction (III) of Scheme 1, since the diffusion of bulky *t*BuOH molecules through the zeolite pores to the active sites is now hindered dramatically by octyl silyl ether species, which are also rather bulky. As a result, *t*BuOH dehydration into butene and water

proceeds under steady-state conditions only on the external surface of H-ZSM-5 crystallites.[3] Thus, octyl silyl ether chemisorbed in the zeolite pores plays the role (in terms of applied catalysis) of "coke", which poisons the H-ZSM-5 catalyst.

Processing of hydrocarbons: As mentioned above, fluxional octyl silyl ether can be formed not only during *t*BuOH dehydration, but also upon oct-1-ene adsorption on the H-ZSM-5 catalyst. It is therefore also expected to play some role in the conversion of hydrocarbon feedstocks on H-ZSM-5. At low temperature (below 373 K) fluxional octyl silyl ether is expected to poison H-ZSM-5 catalysts, like it does during *t*BuOH dehydration. However, the data presented here suggest that at more elevated temperature it (as well as fluxional alkyl silyl ethers with lower or shorter hydrocarbon skeletons) may become involved in the main reaction stream as a key intermediate through which paraffins and aromatics are formed.

Conclusion

Using in situ ^{13}C solid-state MAS NMR in combination with ex situ GC–MS, we have characterized the hydrocarbon products that are formed in the pores of H-ZSM-5 zeolite upon *tert*-butyl alcohol dehydration at 296–673 K in samples with comparable concentrations of adsorbed alcohol and catalytically active Al-OH-Si sites. The following conclusions have been drawn on the nature, composition, structure, and transformations of these products:

1) At 296 K the main hydrocarbon products are adsorbed butene dimers with predominantly linear structure, despite the fact that the initial alcohol had a highly branched structure. The dimers exist in the zeolite pores as a mixture of octene, octyl silyl ether, and octyl carbenium ion; octyl silyl ether is the main adsorption form. The driving force for the formation of linear (rather than branched) dimers is the shape-selectivity effect induced by the small size (ca. 5.5 Å) of the zeolite channels. The vehicle of isomerization of the branched species into the linear ones is the rapidly isomerizing carbenium ion state of adsorbed dimers and their adsorbed butene precursors. Traces of the adsorbed light paraffins are also detected among the reaction products at 296 K, formed by cracking of the adsorbed butene dimers.
2) At 373 K cracking of the adsorbed butene dimers becomes more pronounced. According to ^{13}C NMR spectra, the average length of hydrocarbon skeleton decreases and more adsorbed paraffins are formed. Isobutane is blown out of the zeolite pores with the flow of helium and is clearly detected by GC–MS.
3) At 448 K the adsorbed C_3–C_{7+} paraffins become the dominant hydrocarbon products observed by both in situ ^{13}C NMR and ex situ GC–MS. Simultaneously a mixture of adsorbed polyenes is formed. According to ^{13}C NMR spectra, polyenes exist in the zeolite pores in the form of rather stable cyclopentenyl cations.
4) At 573–673 K adsorbed cyclopentenyl cations further transform into a mixture of condensed and simple aromatics and then into xylenes and toluene. Simultaneously, paraffins crack further to give mainly C_3–C_4 species at 573 K and mainly propane at 673 K.
5) Under practical steady-state conditions in a flow reactor the concentration of reactant in the feedstock stream considerably exceeds that of catalyst active sites and *t*BuOH dehydrates below or near 373 K on H-ZSM-5 zeolite mainly into butenes and water. Here, the fluxional octyl silyl ether is expected to act as a poison that blocks the active catalytic Al-OH-Si sites both chemically and sterically.
6) In conversions of hydrocarbon feedstocks below 373 K, octyl silyl ether (if formed) is also expected to poison H-ZSM-5 catalysts. However, at more elevated temperature it (as well as fluxional alkyl silyl ethers with longer or shorter hydrocarbon skeleton) should become involved in the main reaction stream as key intermediates through which paraffins and aromatics are formed.

Experimental Section

Samples preparations: H-ZSM-5 zeolite (Si/Al = 44, concentration of the strongly acidic Al-OH-Si groups ca. 350 $\mu mol\,g^{-1}$) was synthesized according to ref. [70] Approximately 0.3 g of the zeolite was placed into a glass tube and further activated for 1.5 h in air and 3–4 h under vacuum (10^{-5} torr) at 723 K. After cooling the zeolite sample to room temperature, approximately 300 $\mu mol\,g^{-1}$ of *t*BuOH were adsorbed on it at 296 K. Thus, the ratio of the concentrations of the adsorbed *t*BuOH and acidic Al-OH-Si groups was about 1:1. For NMR experiments *t*BuOH, labeled with ^{13}C isotope in the COH group ([2-^{13}C]*t*BuOH], 82% ^{13}C enrichment) was used. The zeolite sample with adsorbed alcohol was then sealed off from the vacuum system and retained at 296 K or heated for a certain period of time at 373–673 K. Before NMR or thermodesorption experiments, the glass tube with the sample was cooled back to room temperature, opened, and the zeolite sample with adsorbed reaction products was transferred in air into a special container for a thermodesorption experiment or into a 7 mm zirconia NMR rotor for NMR experiment (vide infra). We also performed NMR experiments, where the zeolite sample was not exposed to air. For this purpose around 0.1 g of the zeolite sample was placed into a glass tube, which, after *t*BuOH adsorption and sealing off from the vacuum system, could be tightly packed into the zirconia rotor [71]. We found no difference in the NMR spectra for the samples that had or had not been exposed to air.

Thermodesorption experiments: In these experiments the reaction products desorbed from the zeolite were concentrated in a focusing capillar at 77 K [72]. The experimental setup is shown in Figure 1. The glass container (10 × 4 mm i.d.) with the zeolite sample was placed into the heated section (desorber) of the gas chromatograph injector. In the desorption mode, the carrier gas (helium) was passed through the top of the desorber, and the desorbed vapor streamed out of the chamber to the cryofocusing capillary, where it condensed on cold walls. The setup was then switched to the analysis mode. In this mode, the carrier stream was injected into the bottom part of the desorber body. The focused mixture of organic compounds was then heated, and separated in the capillary column. A combination of the cryofocusing procedure with subsequent separation of the desorbed organics with the capillary column allowed: 1) very low concentrations of the desorbed organics to be measured (starting with $10^{-11}\,g\,cm^{-3}$ of the zeolite) and 2) a better separation of the mixture of the desorbed organics. The temperature of the chamber with the zeolite sample was 296, 373, or 448 K; the stream of helium flowed through at $5\,mL\,min^{-1}$; the desorption time was 30 min.

For the separation of a condensed mixture of hydrocarbons desorbed from the zeolite, a silica fused capillary column of 0.3 mm diameter (i.d.) and 30 m length with SE-30 liquid phase was used. The separation conditions were as follows: 3 min at 323 K, then the programmed increase of temperature ($8\,K\,min^{-1}$) up to 473 K. A 70-70HS "VG" mass spectrometer (MS) was used as the GC detector. Temperature of the MS source was 478 K, scan rate 1.5 s per spectrum, accelerating voltage 2.6 kV. The mass spectra obtained were identified with the aid of a library search procedure. With our GC–MS thermodesorption device we could detect hydrocarbons with four and more carbon atoms. C_1–C_3 hydrocarbons could not be detected.

^{13}C NMR measurements: ^{13}C NMR spectra with magic-angle spinning (MAS) with or without cross- polarization (CP) and with high-power proton decoupling were recorded at 100.613 MHz (magnetic field of 9.4 Tesla) on a Bruker MSL-400 spectrometer at 296 K. The following conditions were used for recording MAS spectra with CP: proton high-power decoupling field was 12 G (4.9 μs 90° ^1H pulse), contact time 5 ms at Hartmann–Hahn matching conditions 51 kHz, delay time between scans 3 s, spinning rate 2.4–3.3 kHz, number of scans 600–15000.

Measurements of spin–lattice (T_1) and spin–spin (T_2) relaxation times were performed with the use of standard methods [73], and at least 12 delay values were used to characterize each curve. We found that T_2 was within 0.5–1.1 s at 373 and 448 K and 1.0–2.8 s at 296 K for all ^{13}C signals of the organic products formed. Therefore, for quantitative assessment of signal areas, one pulse excitation MAS spectra with high-power proton decoupling were recorded using 45° flip angle pulses of 2.5 μs duration and 10–15 s recycle delay in order to avoid the loss of the ^{13}C signal areas. High-power proton decoupling in these experiments was used only during acquisition time. This eliminates nuclear Overhauser enhancement of the signal areas and allows them to be assessed quantitatively [74].

0947-6539/96/0202-0166 $ 10.00+.25/0 Chem. Eur. J. 1996, 2, No. 2

^{13}C chemical shifts (δ) for carbon nuclei of adsorbed organic species were measured with respect to TMS as the external reference with an accuracy of $\delta = \pm 0.5$. The precision in δ determination of the relative line position was 0.1–0.15 ppm. Heteronuclear 2D *J*-resolved ^{13}C MAS NMR spectra were recorded with the following pulse sequence: 90° (^{13}C)–t_1–180° (^{13}C)/180° (^1H)–t_1–acquisition [21,75,76]. Proton high-power decoupling was used during the second half of the evolution period and acquisition time. The increment in t_1 between experiments was 0.5 ms. The increment in t_1 was synchronized with an integer number of rotor periods. Rate of the sample spinning was 2000 Hz. The length of both ^{13}C and ^1H 90° pulses was 4.9 μs. The number of experiments recorded was 32 with a 4 s recycle delay. 1200 transients were accumulated per experiment. A sweep width in $F1$ dimension was 500 Hz. Free induction decays (FIDs) in $F1$ dimension were zero-filled to 128 points to give digital resolution of 7.8 Hz per point. Gaussian apodization in the $F1$ and $F2$ dimensions and power calculation were used for the data processing, followed by a symmetrization. The temperature of the samples was controlled with BVT-1000 variable-temperature unit.

Acknowledgment: The authors express their sincere thanks to Dr. V. N. Romannikov for the synthesis of the samples of H-ZSM-5 zeolite. This work was supported in part by Grant no. 93-03-4808 from the Russian Foundation for Fundamental Research.

Received: April 10, 1995 [F117]

[1] J. Haber, J. Komorek-Hlodzik, T. Romotowski, *Zeolites* **1982**, *2*, 179–184.
[2] M. T. Aronson, R. J. Gorte, W. E. Farneth, *J. Catal.* **1987**, *105*, 455–468.
[3] C. Williams, M. A. Makarova, L. V. Malysheva, E. A. Paukshtis, E. P. Talsi, J. M. Thomas, K. I. Zamaraev, *J. Catal.* **1991**, *127*, 377–392
[4] M. T. Aronson, R. J. Gorte, W. E. Farneth, D. White, *J. Am. Chem. Soc.* **1989**, *111*, 840–846.
[5] A. G. Stepanov, K. I. Zamaraev, J. M. Thomas, *Catal. Lett.* **1992**, *13*, 407–422.
[6] A. G. Stepanov, A. G. Maryasov, V. N. Romannikov, K. I. Zamaraev, *Magn. Reson. Chem.* **1994**, *32*, 16–23.
[7] C. Williams, M. A. Makarova, L. V. Malysheva, E. A. Paukshtis, K. I. Zamaraev, J. M. Thomas, *J. Chem. Soc. Faraday Trans.* **1990**, *86*, 3473–3485.
[8] M. A. Makarova, E. A. Paukshtis, C. Williams, J. M. Thomas, K. I. Zamaraev, *J. Catal.* **1994**, *149*, 36–51; M. A. Makarova, C. Williams, K. I. Zamaraev, J. M. Thomas, *J. Chem. Soc. Faraday Trans.* **1994**, *90*, 2147–2153.
[9] C. D. Chang, A. J. Silvestri, *J. Catal.* **1977**, *47*, 249.
[10] E. G. Derouane, J. B. Nagy, P. Dejaifve, J. H. C. van Hoof, B. P. Spekman, J. C. Védrine, C. Naccache, *J. Catal.* **1978**, *53*, 40–55.
[11] A. Brenner, P. H. Emmett, *J. Catal.* **1982**, *75*, 410–415.
[12] V. N. Romannikov, V. N. Sidelnikov, K. G. Ione, *React. Kinet. Catal. Lett .* **1985**, *27*, 27–31.
[13] E. A. Lombardo, R. Pierantozzi, W. K. Hall, *J. Catal.* **1988**, *110*, 171–183.
[14] M. W. Anderson, J. Klinowski, *J. Am. Chem. Soc.* **1990**, *112*, 10–16; M. W. Anderson, B. Sulikowski, P. J. Barrie, J. Klinowski, *J. Phys. Chem.* **1990**, *94*, 2730–2734.
[15] J. L. White, N. D. Lazo, B. R. Richardson, J. F. Haw, *J. Catal.* **1990**, *125*, 260–263.
[16] F. G. Oliver, E. J. Munson, J. F. Haw, *J. Phys. Chem.* **1992**, *96*, 8106–8111.
[17] E. J. Munson, A. A. Kheir, N. D. Lazo, J. H. Haw, *J. Phys. Chem.* **1992**, *96*, 7740–7746.
[18] S. N. Vereshchagin, N. N. Shishkina, A. G. Anshits, *Kinet. Katal.* **1991**, *32*, 1436–1440; S. N. Vereshchagin, K. P. Dugaev, N. P. Kirik, N. N. Shishkina, A. G. Anshits, *Catal. Today*, **1995**, *24*, 349–356.
[19] E. Breitmaier, W. Voelter, *^{13}C NMR Spectroscopy, Methods and Applications in Organic Chemistry*, Verlag Chemie, Weinheim, **1978**.
[20] C. E. Bronnimann, G. E. Maciel, *J. Am. Chem. Soc.* **1986**, *108*, 7154–7159.
[21] A. E. Derome, *Modern NMR Techniques for Chemistry Research*, Pergamon Press, Oxford, **1987**, pp. 259–268.
[22] To facilitate ^{13}C NMR analysis, *t*BuOH selectively labeled with ^{13}C isotope in the COH group, [2-^{13}C]*t*BuOH, was used.
[23] A. Pines, M. G. Gibby, J. S. Waugh, *J. Chem. Phys.* **1973**, *59*, 569–590.
[24] R. K. Harris, *Nuclear Magnetic Resonance Spectroscopy. A Physico-Chemical View*, Pitman, London, **1983**, pp. 17, 166.
[25] A. G. Stepanov, M. V. Luzgin, V. N. Romannikov, K. I. Zamaraev, *Catal. Lett.* **1994**, *24*, 271–284.
[26] To identify the isotropic chemical shifts δ for the broad signals the procedure of the variation of the speed of the sample rotation between 1.8–3.3 kHz was employed. The lines that corresponded to isotropic value of δ remained unshifted, while the positions of the spinning sidebands varied within $\delta = 15$ depending on the rotation rate.
[27] G. A. Olah, P. R. Cliffod, Y. Halpern, R. G. Johanson, *J. Am. Chem. Soc.* **1971**, *93*, 4219–4222.
[28] G. A. Olah, G. Liang, *J. Am. Chem. Soc.* **1972**, *94*, 6434–6441.
[29] D. Farcasiu, *J. Chem. Soc. Chem. Commun.* **1994**, 1801–1802
[30] E. J. Munson, T. Xu, J. F. Haw, *J. Chem. Soc. Chem. Commun.* **1993**, 75–76; T. Xu, J. Zhang, E. J. Munson, J. F. Haw, *J. Chem. Soc. Chem. Commun.* **1994**, 2733–2735.
[31] J. C. Rees, D. Whittaker, *J. Chem. Soc. Perkin Trans.* **1980**, *2*, 948.
[32] J. F. Haw, B. R. Richardson, I. S. Oshio, N. D. Lazo, J. A. Speed, *J. Am. Chem. Soc.* **1989**, *111*, 2052–2058.
[33] T. Xu, J. F. Haw, *J. Am. Chem. Soc.* **1994**, *116*, 7753–7759.
[34] T. Xu, J. F. Haw, *J. Am. Chem. Soc.* **1994**, *116*, *10188–10195*.
[35] R. K. Harris, *Nuclear Marnetic Resonance. A Physicochemical View*, Pitman, London, **1983**, p. 99.
[36] L. J. Schwartz, E. Meirovitch, J. A. Ripmeester, J. H. Freed, *J. Phys. Chem.* **1983**, *87*, 4453–4461; M. A. Keniry, Kintanar, R. L. Smith, H. S. Gutowski, E. Oldfield, *Biochemistry* **1984**, *23*, 288–298.
[37] G. E. Maciel, D. W. Sindorf, V. J. Bartuska, *J. Chromatogr.* **1981**, *205*, 438; G. R. Hays, A. D. H. Clague, R. Huis, G. Van der Velden, *Appl. Surf. Sci.* **1982**, *10*, 247–263.
[38] L. M. Sverdlov, M. A. Kovner, E. P. Krainer, *Vibrational Spectra of Polyatomic Molecules*, Nauka, Moscow, **1972** (in Russian).
[39] J. P. van den Berg, J. P. Wolthuizen, A. D. H. Clague, G. R. Hays, R. Huis, J. H. C. van Hooff, *J. Catal.* **1983**, *80*, 130–138.
[40] G. A. Olah, D. J. Donovan, *J. Am. Chem. Soc.* **1977**, *99*, 5026–5039.
[41] A. G. Stepanov, V. N. Romannikov, K. I. Zamaraev, *Catal. Lett.* **1992**, *13*, 395–405.
[42] G. A. Olah, *Angew. Chem. Int. Ed. Engl.* **1973**, *12*, 173–212.
[43] M. Saunders, P. Vogel, E. L. Hagen, J. Rosenfeld, *Acc. Chem. Res.* **1973**, 53–59.
[44] B. V. Liengme, W. K. Hall, *Trans. Faraday Soc.* **1966**, *62*, 3229–3243.
[45] N. D. Lazo, B. R. Richardson, P. D. Schettler, J. L. White, E. J. Munson, J. F. Haw, *J. Phys. Chem.* **1991**, *95*, 9420–9425.
[46] A. G. Stepanov, K. I. Zamaraev, *Catal. Lett.* **1993**, *19*, 153–158.
[47] J. Sommer, M. Hachoumy, F. Garin, D. Barthomeuf, *J. Am. Chem. Soc.* **1994**, *116*, 5491–5492; J. Sommer, M. Hachoumy, F. Garin, D. Barthomeuf, J. Vedrine, *ibid.* **1995**, *117*, 1135–1136.
[48] J. Engelhardt, W. K. Hall, *J. Catal.* **1995**, *151*, 1–9.
[49] G. M. Kramer, G. B. McVicker, J. J. Ziemiak, *J. Catal.* **1985**, *92*, 355–363.
[50] A. G. Stepanov, M. V. Luzgin, V. N. Romannikov, K. I. Zamaraev, *J. Am. Chem. Soc.* **1995**, *117*, 3615–3616.
[51] G. A. Olah, E. B. Baker, J. C. Evans, W. S. Tolgyesi, J. S. McIntyre, I. J. Bastein, *J. Am. Chem. Soc.* **1964**, *86*, 1360–1373; G. A. Olah, J. R. DeMember, A. Commeyras, J. L. Bribes, *ibid.* **1971**, *93*, 459–463.
[52] L. J. Bellamy, *Advances in Infrared Group Frequencies*, Methuen, England, **1968**.
[53] V. Stubican, R. Roy, *J. Am. Ceram. Soc.* **1961**, *44*, 625–627.
[54] V. B. Kazansky, I. N. Senchenya, *J. Catal.* **1989**, *119*, 108–126; V. B. Kazansky, *Acc. Chem. Res.* **1991**, *112*, 379–383.
[55] To substantiate this conclusion quantitatively a theoretical analysis is now in progress at our institute.
[56] G. T. Kokotailo, S. L. Lawton, D. H. Olson, M. Meier, *Nature (London)* **1978**, *272*, 437–438; E. M. Flanigen, J. M. Bennett, R. W. Grose, J. P. Cohen, R. L. Patton, R. M. Kirchner, J. V. Smith, *ibid.* **1978**, *271*, 512–516.
[57] C. N. Satterfield, *Heterogeneous Catalysis in Practice*, Moscow, Mir, **1984**, p. 202 (in Russian).
[58] J. Datka, *Zeolites*, **1981**, *1*, 113–116; J. Datka, in *Catalysis on Zeolites* (Eds: D. Kalló, Kh. M. Minachev), Akadémia Kiadó, Budapest, **1988**, pp. 467–487.
[59] J. Nováková, L. Kubelková, Z. Dolejšek, P. Jíru, *Collect. Czech. Chem. Commun.* **1979**, *44*, 3341–3345.
[60] V. Bolis, J. C. Vedrine, J. P. Van de Berg, J. P. Wolthuizen, E. G. Derouane, *J. Chem. Soc. Faraday Trans.* 1, **1980**, *76*, 1606–1616.
[61] H. Forster, J. Seebode, *Proc. Int. Symp. Zeolite Catal.*, Siofok, Hungary, **1985**, p. 413.
[62] A. K. Ghosh, R. A. Kydd, *J. Catal.* **1986**, *100*, 185–195.
[63] A. V. Demidov, A. A. Davydov, L. N. Kurina, *Izv. Akad. Nauk. SSSR, Ser. Khim.* **1989**, *6*, 1229–1233; A. V. Demidov, T. A. Kazantseva, A. A. Davydov, *Zh. Fiz. Khim.* **1990**, *64*, 259–262.
[64] E. A. Lombardo, J. M. Dereppe, G. Marcelin, W. K. Hall, *J. Catal.* **1988**, *114*, 167–175.
[65] E. G. Derouane, J.-P. Gilson, J. B. Nagy, *Zeolites* **1982**, *2*, 42–46.
[66] J.-P. Lange, A. Gutsze, J. Allgeier, H. G. Karge, *Appl. Catal.* **1988**, *45*, 345–356.
[67] A. M. Butlerov, *Zh. Russ. Fiz. Khim. Obstch.* **1877**, *9*, 38 (in Russian)
[68] V. N. Ipatieff, H. Pines, *J. Org. Chem.* **1936**, *1*, 464; H. Pines, *The Chemistry of Catalytic Hydrocarbon Conversions*, Academic Press, New York, **1981**.
[69] N. C. Deno, D. B. Boyd, J. D. Hodge, C. U. Pittman, Jr., J. O. Turner, *J. Am. Chem. Soc.* **1964**, *86*, 1745–1748.
[70] V. N. Romannikov, V. M. Mastikhin, S. Hocevar, V. Drzaj, *Zeolites*, **1983**, *3*, 311–320.
[71] T. A. Carpenter, J. Klinowski, D. T. B. Tennakoon, C. J. Smith, D. C. Edwards, *J. Magn. Reson.* **1986**, *68*, 561.
[72] T. A. Brettell, R. L. Grob, *Int. Laboratory* **1986**, *16*, 30–44.
[73] T. C. Farrar, E. D. Becker, *Pulse and Fourier Transform NMR. Introduction to Theory and Methods*, Academic Press, New York and London, **1971**.
[74] R. K. Harris, *Nuclear Magnetic Resonance Spectroscopy. A Physico-Chemical View*, Pitman, London, **1983**, pp. 107–113.
[75] M. W. Anderson, J. Klinowski, *Chem. Phys. Lett.* **1990**, *172*, 275–278.
[76] A. G. Stepanov, V. N. Zudin, K. I. Zamaraev, *Solid State NMR* **1993**, *2*, 89–93.